journal

J. Am. Ceram. Soc., 94 [10] 3327–3334 (2011)
DOI: 10.1111/j.1551-2916.2011.04612.x

Phase Evaluation in Al_2O_3 Fiber-Reinforced Ti_2AlC During Sintering in the 1300°C–1500°C Temperature Range

C. B. Spencer,[‡] J. M. Córdoba,[§] N. Obando,[¶] A. Sakulich,[‡] M. Radovic,[¶,†] M. Odén,[‖] L. Hultman,[‖] and M. W. Barsoum[‡]

[‡]Department of Materials Science & Engineering, Drexel University, Philadelphia, Pennsylvania, 19104 U.S.A.

[§]Nanostructured Materials, Department of Physics (IFM), Linköping University, 58183 Linköping, Sweden

[¶]Department of Mechanical Engineering, Texas A&M University, College Station, Texas 78843 U.S.A.

[‖]Thin Film Physics Division, Department of Physics, IFM Linköping University, 58183 Linköping, Sweden

In this article, the reactivity of Ti_2AlC powders, with 3 and 10 μm alumina, Al_2O_3, fibers during pressure-assisted sintering is explored. Samples were fabricated by hot-isostatic-pressing (HIPed) or hot-pressing (HPed), and characterized by X-ray diffraction, differential thermal analysis, and electron microscopy—both scanning and transmission—equipped with energy dispersive X-ray spectroscopes. Samples prepared at 1300°C were fully dense, with no apparent reaction between fiber and matrix. In samples HPed to 1500°C, even pure Ti_2AlC powders dissociated to Ti_3AlC_2 according to: 2 Ti_2AlC = Ti_3AlC_2 + $TiAl_x$ (*l*) + (1-*x*) Al (*l*/*v*), with $x < 1$. More severe Al loss results in the formation of TiC_y. The presence of the Al_2O_3 fibers delayed densification enough to allow most of the Al and some of the Ti to escape into the vacuum of the hot press or react with the encapsulating glass during HIPing a resulting in a more intensive dissociation of the Ti_2AlC. Although, in principle Ti_2AlC can be reinforced with Al_2O_3 fibers, the processing/use temperature will have to be kept below 1500°C, as, at that temperature the fibers, used here, sinter together.

I. Introduction

The MAX phases, named for their general formula of $M_{n+1}AX_n$ (where M is an early transition metal, A is an A-group—mostly group 13 and 14—elements, X is either a C and/or N and n = 1,2,3) are a group of nanolayered ternary carbides and nitrides.[1–4] These phases have a hexagonal unit cell (space group $P6_3/mmc$), with two formula units per unit cell, where $M_{n+1}X_n$ layers are interleaved with pure A-group layers.[5] To date, about 50 of M_2AX,[6] 5 M_3AX_2,[7-11] and 7 M_4AX_3,[9,12–18] phases have been identified and synthesized using different techniques. The MAX phases possess an unusual, and sometimes unique, combination of ceramic and metallic properties. Similar to their corresponding binary carbides and nitrides, they are elastically stiff, have relatively low thermal expansion coefficients, good thermal and electrical conductivities, and are resistant to chemical attack.[5] However, unlike their binary counterparts, they are relatively soft (1–5 GPa) and machinable, damage- and thermal-shock resistant.[5,19] Some are also fatigue-, creep-, and oxidation-resistant.[20,21]

Among the MAX phases, Ti_2AlC is considered a good candidate for high-temperature structural applications because of its good high-temperature mechanical properties, excellent oxidation resistance, ease of machinability, and commercial availability. Like other MAX phases, Ti_2AlC is relatively soft, with hardness values of 4.5–5.5 GPa. Its room temperature electrical and thermal conductivities are $\approx 2.7 \times 10^6$ Sm^{-1},[22,23] and 33 to 46 $W\cdot(m\cdot K)^{-1}$.[22,24] Its Poisson's ratio, Young's, shear and bulk moduli are 0.19, 277 GPa, 118 GPa, and 186 GPa, respectively.[25,26]

In early work, the room temperature compressive strength of Ti_2AlC fabricated by a reactive hot-isostatic pressing (HIPing) method at 1600°C was reported to be 540 MPa.[22] Above ≈1000°C, the deformation of Ti_2AlC is plastic (not ductile) and strongly strain rate-dependent. Its "yield" point decreases from 435 MPa at 1000°C to 270 MPa at 1300°C.[22,23] Wang *et al.* recently reported compressive strengths of 670 MPa, flexural strength of 384 MPa, fracture toughness values of 7.0 MPa-$m^{0.5}$ and Vickers hardness values between 4.2 and 5.7 GPa for hot pressed, HPed, Ti_2AlC.[27] Samples, HPed at 1350°C, to a relative density of 98%, and pressureless sintered at 1400°C, to a relative density of 94%, were compared by Hashimoto *et al.*[28] The room temperature fracture toughness and Vickers hardness values of the former were 4.3 MPa-$m^{0.5}$ and 4.2 GPa, respectively. The latter showed higher values of fracture toughness (5.2 MPa-$m^{0.5}$) and lower Vickers hardness values (2.8 GPa).[28]

Despite its potential for use as a high-temperature structural material, surprisingly no results exist on its creep behavior. The only information in the open literature on the creep of the MAX phases consists of publications by Radovic *et al.* and Zhen *et al.* who studied the creep of both coarse- and fine-grained Ti_3SiC_2 in tension and compression.[29–31] In all cases, the dominant creep mechanism is dislocation creep, combined with the generation of large internal stresses as a result of its high plastic anisotropy.[32] Based on the chemical and structural similarities of Ti_2AlC and Ti_3SiC_2, it is reasonable to assume the creep properties of the former are comparable to the latter. In other words, a high tolerance to damage accumulation, dislocation creep with a low, viz. 2, stress exponent, etc.[30]

The attractiveness of Ti_2AlC for high temperature applications, however, derives mostly from its superb oxidation resistance.[33,34] Early work on the oxidation behavior of Ti_2AlC,[35,36] showed that oxidation occurred by the inward diffusion of oxygen and the outward diffusion of Al^{3+} and Ti^{4+} ions through a $(Ti_{1-y}Al_y)O_{2-y/2}$ oxide surface layer and

Y. Zhou—contributing editor

Manuscript No. 29292. Received February 05, 2011; approved April 06, 2011.

This work was funded by the Army Research Office (W911NF-07-1-0628), the Metals Division of the NSF (SGER 0736218), the Air Force Office of Scientific Research (FA9550-09-1-0686), and the Swedish Foundation for Strategic Research (SSF).

[†]Author to whom correspondence should be addressed. e-mail: mradovic@tamu.edu

Report Documentation Page

Form Approved
OMB No. 0704-0188

1. REPORT DATE	2. REPORT TYPE	3. DATES COVERED
2011		**00-00-2011 to 00-00-2011**

4. TITLE AND SUBTITLE	5a. CONTRACT NUMBER
Phase Evaluation in Al2O3 Fiber-Reinforced Ti2AlC During Sintering in the 1300 degrees C-1500 degrees C Temperature Range	5b. GRANT NUMBER
	5c. PROGRAM ELEMENT NUMBER
6. AUTHOR(S)	5d. PROJECT NUMBER
	5e. TASK NUMBER
	5f. WORK UNIT NUMBER
7. PERFORMING ORGANIZATION NAME(S) AND ADDRESS(ES) **Texas A&M University,Department of Mechanical Engineering,College Station,TX,77843**	8. PERFORMING ORGANIZATION REPORT NUMBER
9. SPONSORING/MONITORING AGENCY NAME(S) AND ADDRESS(ES)	10. SPONSOR/MONITOR'S ACRONYM(S)
	11. SPONSOR/MONITOR'S REPORT NUMBER(S)

12. DISTRIBUTION/AVAILABILITY STATEMENT
Approved for public release; distribution unlimited

13. SUPPLEMENTARY NOTES

14. ABSTRACT

15. SUBJECT TERMS

16. SECURITY CLASSIFICATION OF:			17. LIMITATION OF ABSTRACT	18. NUMBER OF PAGES	19a. NAME OF RESPONSIBLE PERSON
a. REPORT	b. ABSTRACT	c. THIS PAGE			
unclassified	**unclassified**	**unclassified**	**Same as Report (SAR)**	**8**	

that the oxidation kinetics were parabolic up to 1100°C at short times (up to 20 h). Wang and Zhou reported that Ti_2AlC follows a cubic oxidation law in the 1000°–1300°C range, where scale growth was governed by oxygen grain-boundary transport.[33] The scales reported by Wang and Zhou were fully dense, adherent, and resistant to thermal cycling.[34] Sundberg *et al.* showed that dense, crack-free stable and protective alumina, Al_2O_3, scales form on Ti_2AlC surfaces. These scales did not spall off even after 8000 thermal cycles from 1350°C to room temperature.[34] The remarkable thermal cycling resistance of the protective oxide scale is attributed to the fact that the thermal expansion coefficient values of Ti_2AlC (8.2×10^{-6} K^{-1})[22] and Al_2O_3 are quite similar. Lastly, Byeon *et al.*[37] confirmed that the compressive residual stresses formed during the oxidation of Ti_2AlC are small. They also demonstrated that the oxidation and spallation resistance of Ti_2AlC were comparable, and sometimes, even better than those of the best-known alumina-forming materials currently available.

Despite these attractive attributes, it is reasonable to expect further improvement in high-temperature mechanical properties of Ti_2AlC by reinforcing it with ceramic fibers. A natural choice of reinforcement is alumina fibers as previous work showed that Ti_2AlC does not react with alumina. Hashimoto *et al.*[28] reported on the mechanical properties of pressureless sintered 5 vol% Al_2O_3–Ti_2AlC composites, and concluded that the addition of Al_2O_3 increased the hardness with no significant changes in room temperature flexural strengths. Zhang *et al.* synthesized *in situ* Ti_2AlC–TiC–Al_2O_3 composites and showed that the composite's hardness increased, while its flexural strengths decreased with increases in the size of the Al_2O_3 particles formed.[38] The addition of 10 vol% α-Al_2O_3, enhanced the strength of Ti_3AlC_2 in the brittle mode of failure (i.e., $T < 1000$°C).[39] However, at $T > 1000$°C, where the failure was more ductile, softening of the matrix resulted in little or no improvement in compressive strengths. The reaction path and room temperature mechanical properties of Ti_3AlC_2/TiC/Al_2O_3 composites processed by combustion sintering of TiO_2, Al, and C powders showed the composites to be harder and stronger than pure Ti_3AlC_2. Their fracture toughness, however, was slightly lower.[40]

To the best of our knowledge, there are no reports on the reactivity of Ti_2AlC with Al_2O_3 fibers. The only study on fiber-reinforced MAX phases is that of a recent article in which we reinforced Ti_2AlC and Ti_3SiC_2 with SiC fibers and showed that the latter cannot be used to reinforce Ti_2AlC matrices made with currently commercially available powders because, they react together to form $Ti_3(Al_{1-x},Si_x)C_2$ solid solutions.[41] The same study, however, showed that SiC fibers can be used to reinforce Ti_3SiC_2. The purpose of this study was to explore the reactivity of Al_2O_3 fibers with commercially available Ti_2AlC powders and to delineate the processing parameters needed to fabricate fully dense composites.

II. Experimental Details

(1) Synthesis

A -325 mesh Ti_2AlC powder [3-ONE-2, Voorhees, NJ] was used for all samples. Two types of Al_2O_3 fibers were used: 10 μm diameter [Nextel™ 610; 3M, St. Paul, MN, composition: >99% Al_2O_3] and ≈3 μm diameter [ALBF1; Zircar Ceramics, Florida, NY, composition: 97% Al_2O_3 and 3% SiO_2] fibers. In both cases, the fibers were chopped with a razor blade into ≈5 cm lengths. Mixing of the powder and fiber was carried out in four ways: (i) *in situ* layering of powder layers, interspersed with layers of chopped fiber; (ii) dry mixing by shaking in a plastic bottle; (iii) dispersing the powders and fibers in an ethanol solution, with a magnetic stirrer; (iv) dispersing in an ethanol solution by mixing in a plastic bottle placed on a ball mill (without balls), for ≈12 h before drying. Based on our results, no discernable differences between the mixing methods were found in the final products and thus are not discussed further.

Prior to HIPing, the mixed dried powders—with various volume fractions, v_f, of alumina fibers (Table I)—were loaded in a steel die and compressed to loads corresponding to stresses of 57 or 97 MPa for 60 s into 12.5 mm^2 × 70 mm^2 bars or 25 mm diameter disks, respectively. On an as-needed basis, small amount of polyvinyl alcohol was added as a binder to enhance the strength of the green bodies. The latter were then embedded in a bed of borosilicate glass (Fisher Scientific, Pittsburgh, PA) in the HIP. The latter (Flow Autoclave Systems Inc., Columbus, OH) was then sealed and the temperature ramped to 750° or 850°C at 10°C/min, then subsequently ramped to 850° or 1000°C at 2.5°C/min and 5°C/min, respectively. These temperatures were held for 60 min, before pressurizing with Ar. Once pressurized, the temperatures were increased again at 10°C/min up to temperatures of 1300°–1500°C and held at these temperatures for 4 h before cooling. The pressure at temperature was ≈100 MPa.

Additionally, two specimens—a pure Ti_2AlC and one containing 9 vol%, 10 μm chopped *in situ* layered Al_2O_3 fibers—were hot pressed, HPed, in graphite dies using a graphite-heated hot press (Series 3600; Centorr Vacuum Industries, Somerville, MA) under a vacuum of 5.8 Pa. The HP was then heated at 500°C/h to 1500°C and held for 4 h. The load at maximum temperature corresponded to a stress of 20 MPa.

Table I. Summary of Runs Made Herein. Column 1 Lists the Fiber Diameter, 211; Column 2 the mol% of Fibers. The Key to the Label Listed in Column 7 is: 211 (for Ti_2AlC Powder) or Fiber Diameter or DSC, Followed by Fiber Volume Fraction, Followed by Consolidation Method, and Last the Processing Temperature. The Processing Time was 3 or 4 (column 6)

Fiber diameter (μm)	mol%	vol%	Processing method	T (°C)	Time (h)	Label	Major phases present
†	N/A	N/A	HIP	1400	3	211-HP-1400	211
†	N/A	N/A	HP	1500	4	211-HP-1500	312
3	43.5	40	HIP	1300	4	3-40-HIP-1300	211
10	19.6	17	HIP	1300	4	10-17-HIP-1300	211
3	11.6	9	HIP	1500	4	3-9-HIP-1500	312 + TiC
10	11.6	9	HIP	1500	4	10-9-HIP-1500	312
3	50.0	46	HIP	1500	4	3-46-HIP-1500	312
10	50.0	46	HIP	1500	4	10-46-HIP-1500	312 + TiC
10	11.6	9	HP	1500	4	10-9-HP-1500	211 + 312
10‡	25.0	21	DSC	1410	0	DSC-1410	211 + 312 + TiC
10‡	25.0	21	DSC	1550	0	DSC-1550	211 + 312 + TiC

†Ti_2AlC powder only.

‡Fibers were manually crushed, mixed with Ti_2AlC powder and cold pressed into small pellets that were then introduced into the DSC.

(2) Differential Scanning Calorimetry and Thermogravimetry

A 3:1 molar ratio of Ti_2AlC powder and 10 μm Al_2O_3 fibers [Nextel™ 610; 3M composition: >99% Al_2O_3]—pre-crushed in a mortar and pestle—were ball-milled, using alumina balls, for ≈12 h and compacted into green bodies (diam = 13 mm) with a small pellet press. These pressed pellets were then cut to a size of ≈4 mm height by 5 mm diameter, and placed in a combined differential scanning calorimetry (DSC) and thermogravimetric unit [Netzsch-STA 449 C Jupiter®; Netzsch, Selb, Germany] equipped with a mass spectrometer [Netzsch-QMS 403 C Aëolos®; Netzsch] and heated at 20°C/min up to 1410° or 1550°C in an ultra pure He atmosphere.

(3) Characterization

The HIP and HPed samples and those placed in the DSC were powdered, using a diamond-coated needle file, for X-ray diffraction (XRD) [Model 500D; Siemens, Karlsruhe, Germany or PW1729; Philips, Eindhoven, Netherlands]. In most cases, 10 wt% pure silicon, Si, powder was used as an internal standard. Scans were made with Cu$K\alpha$ radiation (40 kV and 30 mA) at rates of 1.2 or 2.4° (2Θ)/min, using steps of 0.02 and 0.04°, respectively. Post DSC, runs were scanned with Cu$K\alpha$ radiation (40 kV and 40 mA) at 0.057° (2Θ)/min. Select runs were scanned from 41 to 48° 2Θ at rates of 0.12° (2Θ)/min, to detect any hints of Al–Ti intermetallics [see Fig. 1(b)].

Samples were also cut with a precision diamond saw [Struers Accutom-5, Westlake, OH], mounted, ground and polished with a diamond suspension. A scanning electron microscope (SEM) [Zeiss Supra 50VP, Thornwood, NY] equipped with energy-dispersive spectroscopy (EDS) [Oxford Inca X-Sight, Oxfordshire, UK] was used for microstructural and elemental analysis. However, it should be emphasized that the atomic percents of O and C as determined by EDS and reported in the reminder of this paper are only approximate. Thus, phase composition was predominately determined based on the Ti:Al ratio from EDS results. Select surfaces were etched with a 1:1:1 ratio of water, concentrated HF and HNO_3 for 5 s and immediately rinsed with water. The microstructure was then viewed under an optical microscope, OM, [Olympus PMG3, Center Valley, PA or Keyence, VHX 600, Woodcliff Lake, NJ].

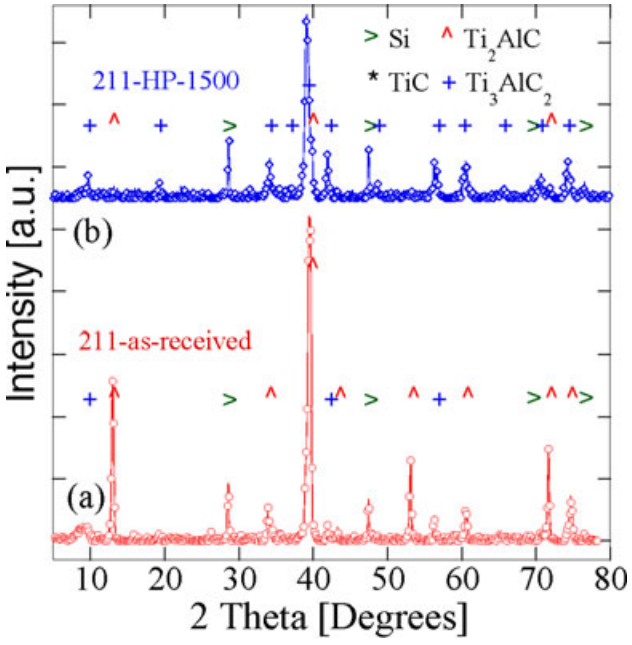

Fig. 1. XRD spectra of (a) as-received Ti_2AlC powder, and (b) sample 211-HP-1500. Pure Si was added as an internal standard and all peaks were normalized to the Si peak at 28.44° 2Θ.

III. Results

(1) Bulk Ti_2AlC

Rietveld analysis of the XRD spectra of the as-received powders (not shown) indicated that it contained ≈14 mol% Ti_3AlC_2 and ≈19 mol% TiC (Table II). Note that these results only quantify the crystalline phases; the presence of XRD amorphous Ti-aluminides (see below) or other phases cannot be ruled out at this juncture.

When the XRD spectrum of the as-received Ti_2AlC powder [Fig. 1(a)] is compared with one after HPing the same powders at 1500°C for 4 h [Fig. 1(b)] it is obvious that Ti_2AlC converts into Ti_3AlC_2. Note that in most XRD spectra, the peak intensities are normalized by the intensity of the internal standard Si peaks and are thus comparable on an absolute scale. A comparison of the two spectra also leaves little doubt that HPing in general reduces the peak intensities.

A typical backscattered electron SEM micrograph [Fig. 2(a)] of the same sample—that was fully dense—showed the presence of two phases. The light gray phase, encompassing ≈96% of the image area, is identified by EDS [Fig. 2(b)] to be Ti_3AlC_2, since the Ti:Al ratio is ≈3.28±0.1 [e.g., points 1, 4, and 6, Fig. 2(b)]. The darker gray, minority phase—making up the remaining ≈4 vol% of the imaged area—is an Al–Ti intermetallic (e.g., points 2, 3, 7, and 8, Fig. 2). At 2.5±0.26, the Al:Ti ratio suggests its chemistry is between $TiAl_2$ and $TiAl_3$. Speckles of a black phase, identified as Al_2O_3, covers less than 1% of the area. In an attempt to find XRD evidence for Ti–Al intermetallics, a slow XRD scan was carried out in the 41–48° 2Θ range of sample 211-HP-1500 (not shown). No peaks belonging to any Ti-aluminide were found suggesting them to be amorphous or at most nano-crystalline.

A typical TEM micrograph of a particle obtained from a sample of Ti_2AlC, without alumina, HPed at 1500°C for 4 h is shown in Fig. 3(a). The EDS confirming the presence of Ti, Al, and C is shown in Fig. 3(b). A selected area diffraction, SAD, of the same particle (inset in Fig. 3) clearly shows the area imaged to be comprised of a large number of nano-grains or domains.

(2) Ti_2AlC/Al_2O_3 Composites

When typical XRD diffractograms of HIPed composite samples are compared (Fig. 4) it is obvious that, here again, HIPing results in: (i) a diminution of the peak intensities belonging to Ti_2AlC; (ii) peak broadening, and (iii) the emergence of peaks belonging to Ti_3AlC_2 and TiC_x [Figs. 4(b)–(d)]. The latter are much more pronounced at 1500°C, than

Table II. Summary of Rietveld Analysis of XRD Results of As-Received Powders and $3Ti_2AlC + Al_2O_3$ Powder Mixture after Heating Twice to 1410° or 1550°C in a DSC at 20°C/min and Immediately Cooling at Same Rate. The goodness of fit, χ^2 is indicated

		Lattice parameter	
Phases	Molar fraction	c (nm)	$a = b$ (nm)
As-received powders			
Ti_2AlC	0.67	1.36946	0.30600
Ti_3AlC_2	0.14	1.8540	0.30652
TiC	0.19	a = 0.43093	
1410°C DSC χ^2 = 2.1			
Ti_2AlC	0.65	1.36711	0.30602
Ti_3AlC_2	0.22	1.85153	0.3709
Al_2O_3	0.13	1.30100	0.7449
1550°C DSC χ^2 = 3.9			
Ti_2AlC	0.65	1.36143	0.30523
Ti_3AlC_2	0.20	1.84585	0.30685
Al_2O_3	0.14	1.29879	0.47552

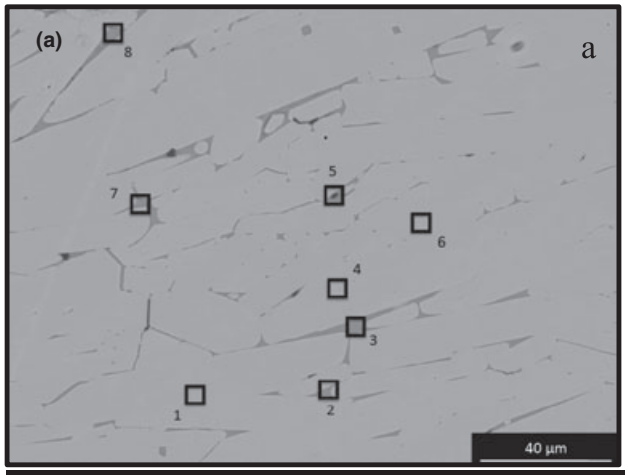

(b) Atomic %

Spot	C	Al	Ti	O	Major Phase
1	29.52	16.39	54.09	-	Ti_3AlC_2
2	11.17	61.87	26.96	-	Al_3Ti
3	9.595	65.46	24.59	-	Al_3Ti
4	29.84	16.42	53.74	-	Ti_3AlC_2
5	4.58	31.75	6.76	56.91	Al_2O_3
6	29.71	16.44	53.85	-	Ti_3AlC_2
7	8.61	62.17	29.22	-	Al_3Ti
8	10.47	64.91	24.62	-	Al_3Ti

Fig. 2. (a) Backscattered electron image of sample 211-HP-1500. (b) EDS results of regions numbered in a. Three phases are present; light gray (Ti_3AlC_2), dark gray (Al_xTi), and black (Al_2O_3).

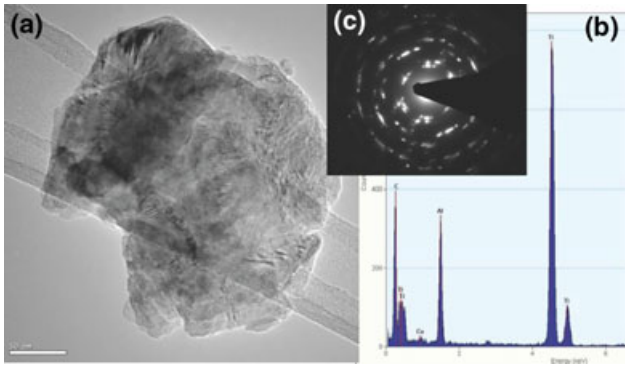

Fig. 3. (a) TEM image of a typical Ti_2AlC particle after heat treatment, showing multiple nanograins. (b) EDS of particle shown in a indicating presence of Ti, Al, and C. Top inset is selected area diffraction of same particle confirming multiplicity of nano grains.

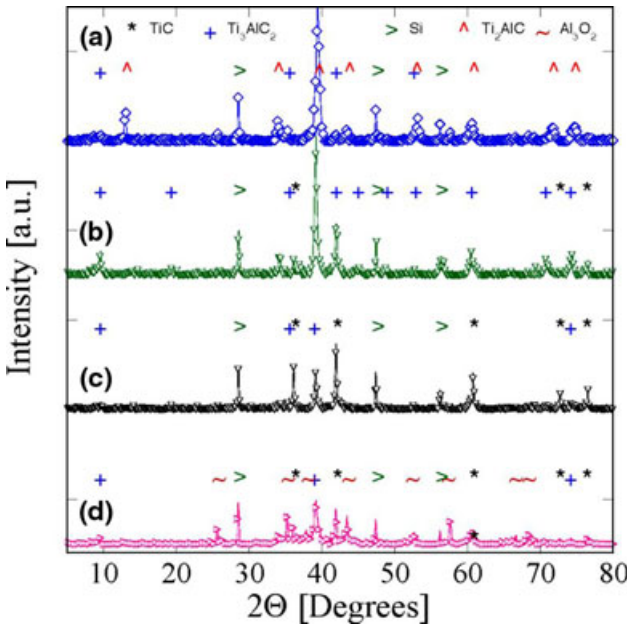

Fig. 4. X-Ray diffraction spectra of samples, (a) 10-17-HIP-1300, (b) 10-9-HIP-1500, (c) 3-9-HIP-1500, and (d) 10-46-HIP-1500. All spectra normalized to 10 wt% Si.

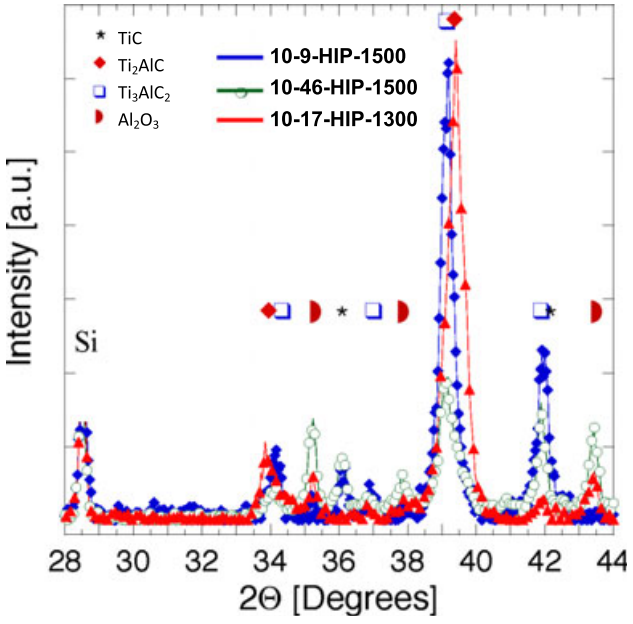

Fig. 5. X-ray diffraction spectra from 28 to 44° 2Θ of samples 10-9-HIP-1500, 10-46-HIP-1500, and 10-17-HIP-1300.

at 1300°C (compare Fig. 4(a) to 4(b) or 4(d) for example). The transformation of the Ti_2AlC in the sample containing 9 vol% fibers is also less intense than the one containing 46 vol% Al_2O_3 fibers.

Confirmation of these conclusions can be found in Fig. 5, in which good quality XRD spectra—from 28 to 44° 2Θ—of samples 10-9-HIP-1500, 10-46-HIP-1500, and 10-17-HIP-1300 are compared. Here again, not only is the 211 phase retained after HIPing at 1300°C for 4 h (red solid diamonds) but, as importantly, the TiC phase present in the starting powder (Table II) disappears.

A polished and etched OM micrograph of sample 3-9-HIP-1500 is shown in Fig. 6(a). Comparing this figure with its XRD spectrum [Fig. 4(c)], three distinct phases can be identified. The white phase is TiC_x, the colored phase is Ti_3AlC_2, and the black phase, which is a minority phase, and barely registers in the XRD pattern, is the Al_2O_3 fibers. In a previous work, we have shown that only when the Ti:A ratio is 3:1 does the etching result in vivid, multicolored grains.[42] We have also repeatedly shown that the easiest method to differentiate between the Ti-containing MAX phases and TiC_y is to etch the samples: the latter shows up as a white or bright phase.[43,44] Consistent with this notion is the polished and etched OM micrograph of sample 10-17-HIP-1300, shown in Fig. 6(b). According to its XRD spectrum [Fig. 4(a)] the majority phase is Ti_2AlC, which turned brown upon etching. The colored phase is Ti_3AlC_2, and the dark, or black, areas are alumina.

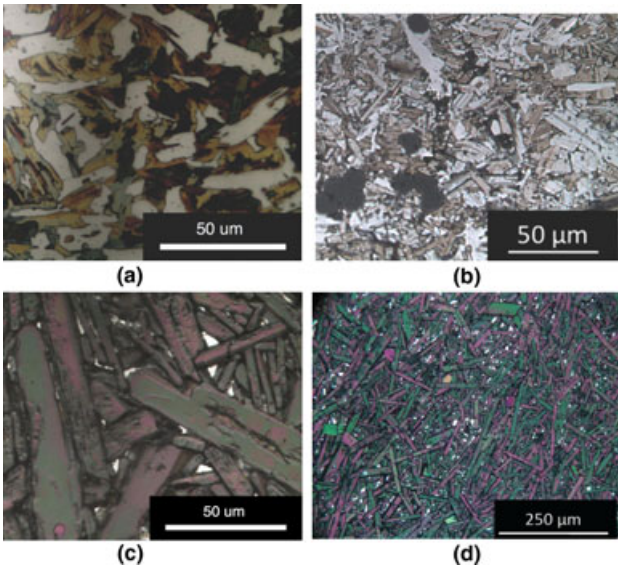

Fig. 6. Polished and etched OM micrographs of sample; (a) 3-9-HIP-1500. The multicolored phase is Ti_3AlC_2; the white phase is TiC_x; the dark regions are either porosity or Al_2O_3 fibers; (b) 10-17-HIP-1300. The majority, brown/beige phase, is Ti_2AlC; the 3 µm diameter Al_2O_3 fibers appear dark gray. (c) and (d) 10-9-HIP-1500 at different magnifications. The majority colored phase is Ti_3AlC_2; the minority white phase, TiC_x.

The polished and etched OM micrographs [Figs. 6(c) and (d)] of sample 10-9-HIP-1500 also confirm the aforementioned observations. Consistent with its XRD pattern [Fig. 4(b)], the colored phase must be Ti_3AlC_2 and the white phase, TiC_x. Note that etching dissolves the Ti-aluminide phases, if present.

Based on backscattered electron SEM images of sample 3-9-HIP-1500 shown in Fig. 7(a) [same as Fig. 6(a)], and the EDS results listed in Fig. 7(b), for the various locations labeled in (a), four phases are identified; Ti_3AlC_2 (pts. 3, 9, and 11), Ti_3C_2 (pts. 7, 8, and 10) Al_2O_3 (pts. 1, 2, and 5), and a Ti–Si phase (pts. 4 and 6). As noted above, the contrast between TiC_x and Ti_3AlC_2 is weak in backscattered mode, which is why it is imperative to combine etched OM micrographs with the latter.

Figure 8(a) shows a low magnification backscattered SEM micrograph of the interface between sample 3-9-HIP-1500 (on right) and borosilicate glass (left). A higher magnification micrograph is shown in Fig. 8(b). EDS of the various numbered regions shown in Fig. 8(b), are listed in Fig. 8(c). Based on these results, the following phases/regions are identified: an Al_2O_3 layer, a boron, B, rich minority phase and borosilicate glass. (The B and C concentrations should not be taken at face value, but are included for the sake of completion). In addition, a bright Ti–Si rich region, similar in composition to the bright areas found in Fig. 7 (e.g., pts. 4 and 6), is present.

Figure 9 shows how the fiber microstructure changes between processing at 1300° (10-17-HIP-1300) and 1500°C (10-46-HIP-1500). When processed at 1300°C [Figs. 9(a)–(c)], the 10 µm Al_2O_3 fibers retain their circular cross section and appear not to have reacted with the matrix as greatly as they do at 1500°C [Fig. 9(d)]. However, even after sintering at 1300°C the Al_2O_3 fibers that were close to each other appear to sinter together, as shown in Fig. 9(b). It is also worth noting, that alumina fibers partially align during cold pressing in a direction perpendicular to the applied load, as can be seen in the sample HIPed at 1300°C [Fig. 9(a)]. However, any alignment of the fibers cannot be observed after HIPing at 1500°C as the fibers sinter together [Fig. 9(d)].

(A) DSC/DTA: The DSC results of the 3:1 molar ratio Ti_2AlC:Al_2O_3 powder mixture heated to 1410°C [Fig. 10(a)]

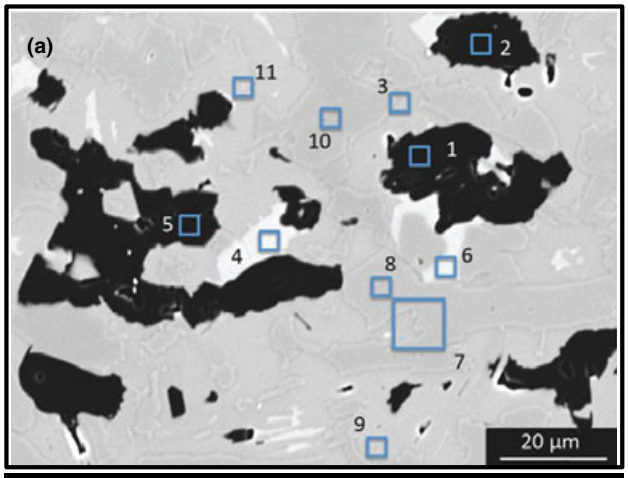

(b) Atomic %

Spot	Al	O	C	Si	Ti	Major Phase
1	37.06	62.94	-	-	-	Al_2O_3
2	37.26	62.84	-	-	-	Al_2O_3
3	9.87	-	34.41	0.59	55.13	Ti_3AlC_2
4	2.86	-	8.11	32.28	56.76	$Ti_2Si(C, Al)$
5	34.29	61.15	2.15	1.15	1.26	Al_2O_3
6	2.5	-	9.46	32.88	55.17	$TiC_{(1-x)}$
7	3.99	-	38.22	-	57.59	$TiC_{(1-x)}$
8	-	-	39.69	-	60.31	$TiC_{(1-x)}$
9	16.08	-	30.76	0.74	52.42	Ti_3AlC_2
10	-	-	38.47	-	61.53	$TiC_{(1-x)}$
11	16.06	-	28.43	0.86	54.66	Ti_3AlC_2

Fig. 7. (a) Backscattered electron, SEM image of sample 3-9-HIP-1500. (b) Summary of EDS results for various locations labeled in (a). Based on the EDS results four phases are identified; Ti_3AlC_2 (pts. 3, 9, and 11), Ti_3C_2 (pts. 7, 8, and 10), Al_2O_3 (pts. 1, 2, and 5), and a Ti-Si phase (pts. 4 and 6). The Si comes from the borosilicate glass used to encapsulate the samples during HIPing (see below).

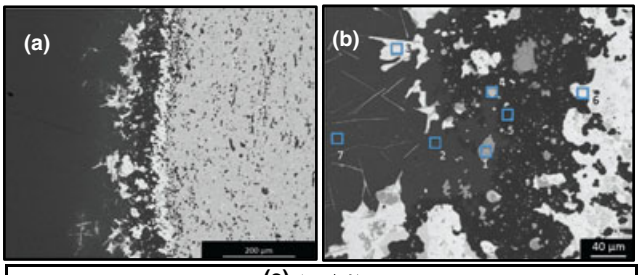

(c) Atomic %

Spot	B	C	O	Na	Al	Si	K	Ti	Phase
1	58.61	4.64	-	-	-	13.3	-	23.46	B rich
2	-	4.85	58.1	6.3	11.17	18.48	1.09	-	O rich
3	-	8.66	-	-	-	36.17	-	55.18	Ti-Si
4	-	8.6	-	-	-	58.73	-	32.68	Ti-Si
5	-	-	60.51	-	39.49	-	-	-	Al_2O_3
6	-	12.73	-	-	1.31	33.9	-	52.05	Ti-Si
7	-	2.49	60.66	4.74	9.29	21.52	1.29	-	Silicate galss

Fig. 8. Backscattered electron SEM micrographs of sample 3-9-HIP-1500 near the borosilicate glass interface at, (a) low magnification, and (b) higher magnification. (c) EDS results of the various numbered locations in the SEM micrograph are listed in the table shown.

are, for the most part, featureless. A small, but observable endothermic event at 1350°C during heating, which is also mirrored upon cooling, can be discerned. The TGA results of the sample heated to 1550°C [Fig. 10(b)] show four regions of mass change: (i) a weight loss during the initial temperature increase; (ii) a gradual mass gain until ≈1475°C, at

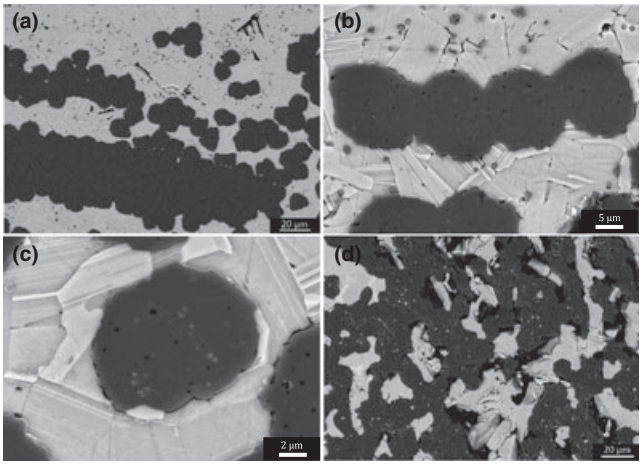

Fig. 9. Backscattered electron SEM images showing effect of temperature on Al_2O_3 fiber morphology, for sample, (a), (b), (c) 10-17-HIP-1300 and, (d) 10-46-HIP-1500. The fibers in a, b, and c retained their shape, while those in b and d agglomerated and sintered together.

which temperature mass is lost; (iii) mass loss continues upon cooling reaching a minimum also ≈1475°C, after which the sample, (iv) gains weight down to ≈800°C, below which it levels off. The concomitant mass spectroscopy results, also shown in Fig. 10(b), indicate the emission of several gaseous products such as CO_2 and CO.

Table II summarizes the Rietveld analysis results of the XRD spectra of the as-received powders and the $3Ti_2AlC + Al_2O_3$ powder mixture after heating twice to 1410° or 1550° C in the DSC at 20°C/min and immediately cooling at the same rate. Only three phases, Ti_2AlC, Ti_3AlC_2, and Al_2O_3 were detected.

IV. Discussion

Based on the results presented above there is little doubt that at 1300°C the Ti_2AlC phase is maintained (solid diamonds in Fig. 5) and that no reaction between the Al_2O_3 fibers and matrix occurs [Figs. 9(a)–(c)]. Upon heating to 1500°C, however, even pure Ti_2AlC converts into Ti_3AlC_2 (Figs. 1 and 2) in a transformation that depends on temperature, time, and "access" of Al to surroundings (see below). The question remaining is: what are the operative reactions? One possibility is for Ti_2AlC to react with the TiC present in the initial powders to form Ti_3AlC_2.[45] It is this reaction that most probably consumes the TiC present in the initial powder and thus explains why neither the samples HIPed at 1300°C (Fig. 4) nor those heated in the DSC (Table II) contained TiC. Note that after heating in the DSC, the 211/312 ratio decreases from ≈5 to 3 (Table II).

The amount of TiC in the initial powder, however, is insufficient to convert all the 211 into 312. At higher temperatures Ti_2AlC transform to Ti_3AlC_2 most probably according to the following reaction:

$$2Ti_2AlC = Ti_3AlC_2 + TiAl_{1-x} + xAl(v \text{ or } l) \quad (1)$$

where $x < 1$. The composition, x, of the intermetallic formed depends on the amount of Al lost to the surroundings. If one mole of Al were lost, pure Ti would remain. However, before this can occur, the continued loss of Al should lead to the formation of TiC_x according to following simplified reaction:

$$Ti_3AlC_2 = 2TiC + Al(v \text{ or } l) + Ti(v) \quad (2)$$

It follows that the presence of TiC in the final composite (Figs. 4(c), 4(d) and 7) is not too surprising.

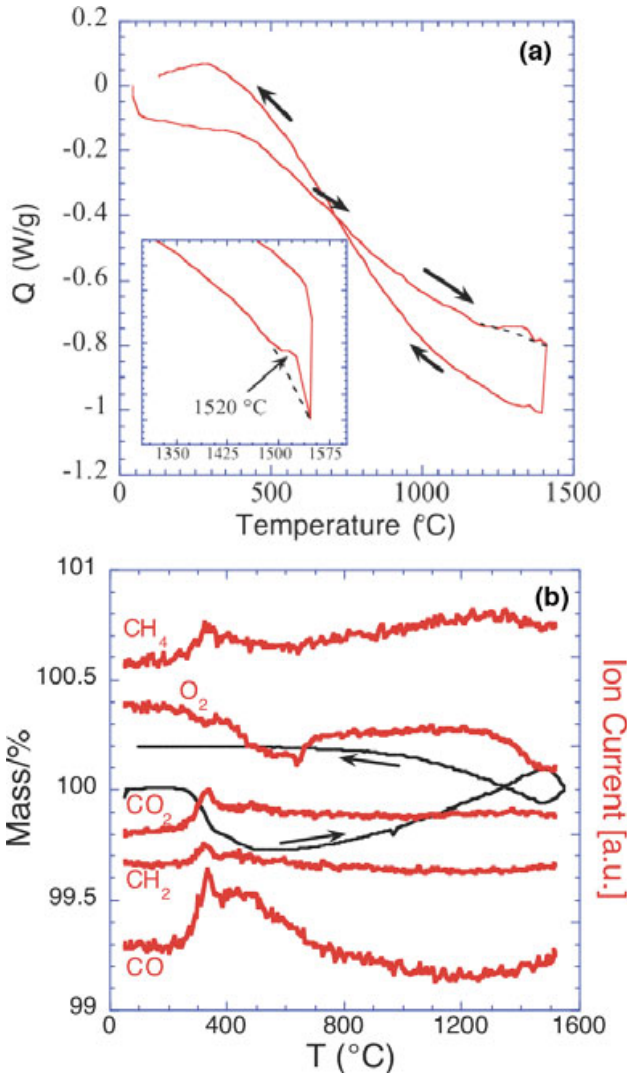

Fig. 10. (a) DSC of $3Ti_2AlC:Al_2O_3$ powder mixture heated to 1410°C. Inset shows DTA results of same composition heated to 1550°C. A broad exothermic peak centered around 1520°C is observed on cooling; (b) TGA of sample heated to 1550°C. Early mass loss is followed by mass gain and ultimately mass loss at $T > 1450$°C. The gases evolved during heating are indicated on the figure.

Reactions 1 and 2 are simplified in the sense that we are not allowing any non-stoichiometry in the Ti_3AlC_2 phase. Based on the various micrographs of the various samples (e.g., Fig. 2) it is clear that the volume fraction of the $TiAl_x$ phase is significantly less than it should be based on reaction 1. And while the exact reason for this state of affairs is not fully understood, one, or more, of the following two arguments can be invoked.

First, the $TiAl_{1-x}$—which is presumably a liquid at 1500°C—is squeezed to the sample's surface, where it reacts with the surrounding glass (see below) in the HIP, or the graphite foil surrounding the samples in the HP. The evaporation of Ti cannot be ruled out at this time.

Second, the Ti_3AlC_2 phase contains excess Ti and possibly C. This conjecture is consistent with the fact that the Ti/Al ratio of the Ti_3AlC_2 phase in Figs. 2 and 7 is closer to 3.3, than it is to 3. Given the difficulty of accurately quantifying the C-content in the EDS, more careful work is needed to explore whether the C/Al ratio also increases. The Ti and C excesses can be explained by Al deficiency in the A-layers, as well as thickening of any TiC_y layers sandwiched between the Ti_3AlC_2 planes. A similar decomposition mechanism was reported for Ti_3SiC_2 (0001) thin films.[46]

The latter conclusion is also in tune with our understanding of how the MAX phases react. Given the chemical stability of the $M_{n+1}X_n$ blocks and the fact that the A-layers are relatively loosely held, by now it is fairly well established that the most common reaction of the MAX phases is the selective loss/reaction of the A-group element. For example the MAX phases do not melt congruently, but decompose peritectically to $M_{n+1}X_n$ and the A-group element. The decomposition temperatures vary over a wide range; from ≈850°C for Cr_2GaN[47] to above 2300°C for bulk Ti_3SiC_2.[48] The decomposition temperatures of the Sn-containing ternaries range from 1200° to 1400°C.[49] Ti_3SiC_2 can be processed at 1600°C in bulk form, but thin epitaxial films lose Si at temperatures as low as 1100°C.[50] Heating Ti_3SiC_2 in a C-rich atmosphere results in the loss of Si and the formation of TiC_x.[50] When the same compound is placed in molted cryolite,[42] or molten Al[51] essentially the same reaction occurs: Si escapes and TiC_y forms.

The effect of temperature on the transformation is best seen in Fig. 4; when the powder was HIPed to 1300°C, there was little change compared with the initial powder [compare Figs. 1(a) and 4(a)]. When the same powder was HIPed or HPed at 1500°C for 4 h, it disassociated to Ti_3AlC_2 [Fig. 1 and Figs. 4(b)–(d)]. However, after the two *rapid* consecutive DSC runs, to 1410° and 1500°C, only a small fraction of the initial Ti_2AlC dissociates.

The evidence for the presence of a Ti-aluminide phase formed according to Equation 1 is multifold. It is clearly seen at the boundaries between the Ti_3AlC_2 grains (Fig. 2). A broad exothermic peak, centered around 1520°C, is observed just upon cooling in the DTA [inset in Fig. 10(a)]. As no peaks belonging to any Ti-aluminide phases were observed in any of the XRD spectra they must be amorphous or nano-crystalline. Finally, a few Ti-rich nanoparticles, that SAD showed to be amorphous (not shown), were imaged in the TEM. In another region, an Al-rich, Ti-aluminide particle was found that was not amorphous. SAD showed it to be the tetragonal intermetallic $Al_{0.64}Ti_{0.36}$ (ICSD-file 50-0726) with lattice parameter, $a = b = 0.40296$ nm; the c lattice parameter was 0.29561 nm.

Using the Scherer formula, the average particle size of the Ti_3AlC_2 phase formed during the DSC run is estimated to be ≈12±3 nm, a conclusion confirmed by TEM (Fig. 3 and its inset). This is an important result as it can both explain the general diminution of the MAX phase peaks upon heating, and suggest a relatively easy method to produce nano-grains of the MAX phases. The very fine nature of the grains that form suggests that they formed by a nucleation and growth process. Had the 211 to 312 transformation occurred by a rearrangement of the number of TiC_x layers in between the Al planes—i.e., by a topotaxial or intergrowth process—larger grains would most probably have formed.

The evidence for the loss of Al from the system is also clear and multifold. Given its low melting point relative to Ti, it is likely that the majority of the weight loss at $T > 1475$°C is due to the loss of Al. In recent experiments, it was noted that when Ti_2AlC powders were heated to 1500°C for 2 h, in a graphite foil-lined alumina boat a yellow cake formed. XRD of the latter showed it to be Al_4C_3. The initial weight loss during heating in Fig. 10(b) is due to the loss of moisture and other adsorbed gases from the powder compact. It is presumably the reaction between moisture and C in the compact that produces CH_4 and CH_2 and CO and CO_2. The weight gain between ≈800° and 1475°C is presumably due to slight oxidation of the powders. Why that increases the oxygen concentration [Fig. 10(b)] however, remains unclear. The relatively sharp mass loss around 1475° C that continues as the sample is cooled [Fig. 10(b)] is also presumably due to the loss of Al from the system. The reason why Al or AlO was not detected by the mass spectrometer [Fig. 10(b)] is most probably due to the condensation of these gases in the tubes connecting the reaction chamber to the mass spectrometer.

Figure 8 not only indicates that the Al is highly mobile, but, as important, that it reacts with the surrounding glass. As alumina is thermodynamically more stable than silica, then the most likely simplified reaction is:

$$\text{boro-silicate glass} + TiAl_{2.5}(l) = Al_2O_3 + TiSi_z \qquad (3)$$

In other words, the Al reduces the Si in the glass. This reaction explains the presence of, almost continuous, layers of both Al_2O_3 and $TiSi_z$ near the glass/sample interface [Figs. 8(a) and (b)]. It also explains the presence of $TiSi_z$ pockets deep within the bulk of the samples [Figs. 7(a) and (b)]. The $TiSi_z$ phase [Fig. 7(a) and Figs. 8(a) and (b)] was most likely liquid when it formed, and penetrated into the sample before it fully densified.

The results presented herein do not necessarily imply that Ti_2AlC does not exist at temperatures > 1400°C. After all the first successful bulk synthesis of this compound was carried out by HPing elemental powders for 4 h at 1600°C.[1] The answer to this apparent paradox, for which there is some confusion in the literature, has to be to do with the free energy change, ΔG, of reaction 1 or one that transforms Ti_2AlC to TiC_x directly. In an open system, where the activity of Al in the surroundings is vanishingly small, ΔG will always be negative at all temperatures. In other words, the MAX phases are only kinetically stable. This is seen here in that the DSC sample rapidly heated to, and cooled from, 1550°C only marginally transformed to Ti_3AlC_2, while the sample heated to 1500°C for 4 h did so much more thoroughly.

This insight also explains why samples in which the volume fraction of fibers was high tended to dissociate more. Presumably the fibers delayed densification long enough to allow most of the Al and possibly Ti to escape into the vacuum of the hot press or react with the encapsulating glass during HIPing. The main evidence for this conjecture can be seen in comparing the SEM micrographs of sample 211-HP-1500 (Fig. 2) and 3-9 HIP-1500 (Fig. 7). In both cases, the major phase present is Ti_3AlC_2; however, with the incorporation of fiber in the latter, no Ti–Al was found within the bulk of the sample. We note in passing that all samples were fully dense after processing; we saw no evidence of macro- or micropores.

The results presented herein suggest that alumina fibers can be used to reinforce Ti_3AlC_2 and/or Ti_2AlC, if the latter does not decompose [Fig. 9(a)]. However, based on this work, 1300°C may be near the maximum processing temperature, not because the fibers react with the matrix—they do not—but because at 1500°C they sinter together [Fig. 9(d)] and presumably lose their load-bearing capabilities. If more stable Al_2O_3 fibers can be found, the results shown here suggest that they can be used to reinforce Ti_2AlC and/or Ti_3AlC_2.

Lastly, it is instructive to compare the results obtained here with those obtained when Ti_2AlC reacts with SiC.[41] The simplified reaction believed to occur there is:

$$2Ti_2AlC + SiC \rightarrow Ti_3SiC_2 + 2Al + TiC$$

In that case, the reaction is exothermic and occurs suddenly at about 1170°C. One hundred degrees later the peak becomes endothermic, presumably due to the egress of the Al from the basal planes and its melting. On cooling, a clear exothermic peak at 680°C—absent here—is observed. Interestingly, EDS of SEM micrographs of the SiC-reinforced samples indicate the presence of a Ti-aluminide phase, quite similar in composition to the one observed here, that presumably results from the Ti_2AlC to Ti_3AlC_2 transformation, viz. reaction 1.

V. Conclusions

Fully dense, alumina fiber-reinforced composites can be fabricated, at temperatures as low as 1300°C, by HIPing or HPing commercially available Ti_2AlC powders with 3–10 μm commercially available alumina fibers for 4 h. At 1500°C, the alumina fibers sinter together and as importantly, the loss of Al to the surrounding results in the dissociation of Ti_2AlC into Ti_3AlC_2 and $TiAl_x$. If the loss of Al is severe, the ultimate phase remaining would be TiC_y. The loss of Ti by evaporation/reaction at 1500°C cannot be ruled out now.

As the MAX phases can only be kinetically stable when heated in an environment in which the activity of the A-element is vanishingly small, it is not surprising that the aforementioned reactions are time, temperature and densification rate dependent. Low temperature, short times and rapid densification decrease the propensity of dissociation at high temperatures.

References

[1]M. W. Barsoum, "The $M_{N+1}AX_N$ Phases: A new Class of Solids; Thermodynamically Stable Nanolaminates," *Prog. Solid State Chem.*, **28** [1–4] 28–01 (2000).

[2]W. Jeitschko, H. Nowotny, and F. Benesovsky, "Kohlenstoffhaltige Ternare Verbindungen (H-Phase)," *Monatsh. Chem.*, **94** [4] 672 (1963).

[3]W. Jeitschko, H. Nowotny, and F. Benesovsky, "Ti2AlN, Eine Stickstoffhaltige H-Phase," *Monatsh. Chem.*, **94** [4] 1198 (1963).

[4]W. Jeitschko, H. Nowotny, and F. Benesovsky, "Carbides Of Formula T_2MC," *J. Less-Comm. Metal*, **7** [4] 133–42 (1964).

[5]M. W. Barsoum, "Physical Properties of the MAX Phases"; in *Encyclopedia of Materials Science and Technology*, Edited by K. H. J. Buschow, R. C. Cahn, M. C. Flemings, B. Ilschner, E. J. Kramer, S. Mahajan, and P. Veyssiere. Elsevier, Amsterdam, 2006.

[6]H. Nowotny, "Struktuchemie Einiger Verbindungen der Ubergangsmetalle mit den Elementen C, Si, Ge, Sn," *Prog. Solid State Chem.*, **5** 27–70 (1971).

[7]S. Dubois, T. Cabioc'h, P. Chartier, V. Gauthier, and M. Jaouen, "A New Ternary Nanolaminate Carbide:Ti_3SnC_2," *J. Am. Ceram. Soc.*, **90** [8] 2642–4 (2007).

[8]W. Jeitschko and H. Nowotny, "Die Kristallstructur von Ti_3SiC_2-Ein Neuer Komplxcarbid-Typ," *Monatsh. Chem.*, **98** [2] 329 (1967).

[9]Z. J. Lin, M. J. Zhuo, Y. C. Zhou, M. S. Li, and J. Y. Wang, "Microstructures and Theoretical Bulk Modulus of Layered Ternary Tantalum Aluminum Carbides," *J. Am. Ceram. Soc.*, **89** [12] 3765–9 (2006).

[10]M. A. Pietzka and J. C. Schuster, "Summary of Constitution Data of the System Al-C-Ti," *J. Phase Equilibria*, **21** [2] 392–400 (1994).

[11]H. Wolfsgruber, H. Nowotny, and F. Benesovsky, "Die Kristallstruktur von Ti3GeC2", *Monatsh. Chem.*, **98** [6] 2403 (1967).

[12]J. Etzkorn, J. M. Ade, D. Kotzott, M. Kleczek, and H. Hillebrecht, "Ti_2GaC, Ti_4GaC_3, and Cr_2GaC–Synthesis, Crystal Growth and Structure Analysis of Ga-Containing MAX-Phases $M_{n+1}GaC_n$ With M=Ti, Cr and n=1,3," *J. Solid State Chem.*, **182** [5] 995–1002 (2009).

[13]H. Hogberg, P. Eklund, J. Emmerlich, J. Birch, and L. Hultman, "Epitaxial Ti_2GeC, Ti_3GeC_2, and Ti_4GeC_3 MAX-Phase Thin Films Grown by Magnetron Sputtering," *J. Mater. Res.*, **20** [4] 779–82 (2005).

[14]C. F. Hu, F. Z. Li, J. Zhang, J. M. Wang, J. Y. Wang, and Y. C. Zhou, "Nb_4AlC_3 – A new Compound Belonging to the MAX Phases," *Scripta Mater.*, **57** [10] 893–6 (2007).

[15]C. F. Hu, J. Zhang, J. M. Wang, F. Z. Li, J. Y. Wang, and Y. C. Zhou, "Crystal Structure of V_4AlC_3: A New Layered Ternary Carbide," *J. Am. Ceram. Soc.*, **91** [2] 636–9 (2008).

[16]J. P. Palmquist, S. Li, P. O. A Persson, J. Emmerlich, O. Wilhelmsson, H. Hogberg, M. I Katsnelson, B. Johansson, O. Eriksson, L. Hultman, and U. Jansson, "$M_{n+1}AX_n$ Phases in the Ti-Si-C System Studied by Thin-Film Synthesis and Ab Initio Calculations," *Phys. Rev. B*, **70** [16] 165401 (2004).

[17]A. T. Procopio, M. W. Barsoum, and T. El-Raghy, "Characterization of Ti_4AlN_3," *Metall. Mater. Trans. A*, **31** [2] 333–7 (2000).

[18]C. J. Rawn, M. W. Barsoum, T. El-Raghy, A. Procipio, C. M. Hoffmann, and C. R. Hubbard, "Structure of Ti_4AlN_3–A Layered $M_{n+1}AX_n$ Nitride," *Mater.Res. Bull.*, **35** [11] 1785–96 (2000).

[19]M. W. Barsoum and M. Radovic, "Mechanical Properties of the MAX Phases"; in *Encyclopedia of Materials Science and Technology*, Edited by R. C. Cahn, K. H. J. Buschow, M. C. Flemings, E. J. Kramer, S. Mahajan, and P. Veyssiere. Elsevier Science, Amsterdam, 2004.

[20]C. J. Gilbert, D. R. Bloyer, M. W. Barsoum, T. El-Raghy, A. P Tomasia, and R. O. Ritchie, "Fatigue-Crack Growth and Fracture Properties of Coarse and Fine-Grained Ti_3SiC_2," *Scripa Mater.*, **42** [8] 761–97 (2000).

[21]H. Zhang, Z. G. Wang, Q. S. Zang, Z. F. Zhang, and Z. M. Sun, "Cyclic Fatigue Crack Propagation Behavior of Ti_3SiC_2 Synthesized by Pulse Discharge Sintering (PDS) Technique," *Scripta Mater.*, **49** [1] 87–92 (2003).

[22]M. W. Barsoum, D. Brodkin, and T. El-Raghy, "Layered Machinable Ceramics For High Temperature Applications," *Scripta Mater.*, **36** [5] 535–41 (1997).

[23]M. W. Barsoum, M. Ali, and T. El-Raghy, "Processing and Characterization of Ti_2AlC, Ti_2AlN, and $Ti_2AlC_{0.5}N_{0.5}$," *Metall. Mater. Trans. A*, **31** [7] 1857–65 (2000).

[24]J. D. Hettinger, S. E. Lofland, P. Finkel, J. Palma, K. Harrell, S. Gupta, A. Ganguly, T. El-Raghy, and M. W. Barsoum, "Electrical Transpot, Thermal Transport and Elastic Properties of M_2AlC (M = Ti, Cr, Nb and V) Phases," *Phys. Rev. B*, **72** [11] 115120 (2005).

[25]M. Radovic, A. Ganguly, M. W. Barsoum, T. Zhen, P. Finkel, S. R. Kalidindi, and E. Lara-Curzio, "On the Elastic Properties and Mechanical Damping of Ti_3SiC_2, Ti_3GeC_2, $Ti_3Si_{0.5}Al_{0.5}C_2$ and Ti_2AlC in the 300-1573 K Temperature Range," *Acta Mater.*, **54** [10] 2757–67 (2006).

[26]B. Manoun, S. K. Saxena, M. W. Barsoum, and T. El-Raghy, "X-ray High-Pressure Study of Ti_2AlN and Ti_2AlC," *J. Phys. Chem. Solid*, **67** [12] 2512–6 (2006).

[27]P. Wang, B.-C. Mei, X. L. Hong, and W. B. Zhou, "Synthesis of Ti_2AlC by hot Pressing and its Mechanical and Electrical Properties," *Trans. Nonferrous Met. Soc. China*, **17** [5] 1001–4 (2007).

[28]S. Hashimoto, M. Takeuchi, K. Inoue, S. Honda, H. Awaji, K. Fukuda, and S. Zhang, "Pressureless Sintering and Mechanical Properties of Titanium Aluminum Carbide," *Mater. Lett.*, **62** [10–11] 1480–3 (2008).

[29]M. Radovic, M. W. Barsoum, T. El-Raghy, and S. M. Wiederhorn, "Tensile Creep of Fine Grained (3-5 um) Ti_3SiC_2 in the 1000–1200°C Temperature Range," *Acta Mater.*, **49** [19] 4103–12 (2001).

[30]M. Radovic, M. W. Barsoum, T. El-Raghy, and S. M. Wiederhorn, "Tensile Creep of Coarse-Grained Ti_3SiC_2 in the 1000–1200°C Temperature Range," *J. Alloy Compds*, **361** [1–2] 299–312 (2003).

[31]T. Zhen, M. W. Barsoum, S. R. Kalidindi, M. Radovic, Z. M. Sun, and T. El-Raghy, "Compressive Creep of Fine and Coarse-Grained T_3SiC_2 in Air in the 1100 to 1300°C Temperature Range," *Acta Mater.*, **53** [19] 4963–73 (2005).

[32]F. Barcelo, S. Doriot, T. Cozzika, M. Le Flem, J. L. Béchade, J.-L. M. Radovic, and M. W. Barsoum, "Electron-Backscattered Diffraction and Transmission Electron Microscopy Microstructural Study of Post-Creep Ti3SiC2," *J. Alloy Compds*, **488** [1] 181–9 (2009).

[33]X. H. Wang and Y. C. Zhou, "High-Temperature Oxidation Behavior of Ti_2AlC in Air," *Oxid. Metals*, **59** [33–4] 303–20 (2003).

[34]M. Sundberg, G. Malmqvist, A. Magnusson, and T. El-Raghy, "Alumina Forming High Temperature Silicides and Carbides," *Ceram. Int.*, **30** [7] 1899–904 (2004).

[35]M. W. Barsoum, "Oxidation of $Ti_{n+1}AlX_n$ Where n = 1-3 and X is C, N, Part I: Model," *J. Electrochem. Soc.*, **148** [8] C544–50 (2001).

[36]M. W. Barsoum, N. Tzenov, A. Procopio, T. El-Raghy, and M. Ali, "Oxidation of $Ti_{n+1}AlX_n$ Where n = 1-3 and X is C, N, Part II: Experimental Results," *J. Electrochem. Soc.*, **148** [8] C551–62 (2001).

[37]J. W. Byeon, J. Liu, M. Hopkins, W. Fischer, N. Garimella, K. B. Park, M. P. Brady, M. Radovic, T. El-Raghy, and Y. H. Sohn, "Microstructure and Residual Stress of Alumina Scale Formed on Ti_2AlC at High Temperature in Air," *Oxid. Metals*, **68** [12] 97–111 (2007).

[38]D. L. Zhang, Z. H. Cai, A. J. Huang, and R. Yang, "Synthesis, Microstructure and Mechanical Properties of a Novel $Ti_2AlC/TiC/Al_2O_3$ in Situ Composite," *J. Am. Ceram. Soc.*, **89** [11] 3325–0 (2006).

[39]J. Chen, M. Liu, Y. Bao, and Y. C. Zhou, "Y. Failure-Mode Dependence of the Strengthening Effect in Ti_3AlC_2/10 vol.% Al_2O_3 Composite," *Int. J. Mat. Res.*, **97** [8] 1708–1 (2006).

[40]J. Chen, M. Liu, and Y. C. Zhou, "In Situ Synthesis of Ti_3AlC_2/TiC-Al_2O_3 Composite," *J. Mater. Sci. Technol.*, **22** [4] 455–8 (2006).

[41]C. B. Spencer, J. M. Córdoba, N. H. Obando, M. Radovic, M. Odén, L. Hultman, and M. W. Barsoum, "The Reactivity of Ti_2AlC and Ti_3SiC_2 with SiC Fibers and Powders up to Temperatures of 1550°C," *J. Am. Ceram. Soc.*, **94**, (2011).

[42]M. W. Barsoum, T. El-Raghy, L. Farber, M. Amer, R. Christini, and A. Adams, "The Topotaxial Transformation of Ti_3SiC_2 To Form a Partially Ordered Cubic $TiC_{0.67}$ Phase by the Diffusion of Si Into Molten Cryolite," *J. Electrochem. Soc.*, **146** [10] 3919–23 (1999).

[43]T. El-Raghy and M. W. Barsoum, "Processing and Mechanical Properties of Ti_3SiC_2: Part I: Reaction Path and Microstructure Evolution," *J. Amer. Cer. Soc.*, **82** [10] 2849–54 (1999).

[44]A. Ganguly, T. Zhen, and M. W. Barsoum, "Synthesis and Mechanical Properties of Ti_3GeC_2 and $Ti_3(Si_xGe_{1-x})C_2$ (x = 0.5, 0.75) Solid Solutions," *J. Alloy. Compds*, **376** [1–2] 287–95 (1999).

[45]E. H. Kisi, E. Wu, J. S. Zobec, J. S. Forrester, and D. P. Riley, "Inter-Conversion of $M_{n+1}AX_n$ Phases in the Ti-Al-C System," *J. Am. Ceram. Soc.*, **90** [6] 1912–6 (2007).

[46]J. Emmerlich, H. Högberg, O. Wilhelmsson, U. Jansson, D. Music, J. M. Schneider, and L. Hultman, "Thermal Stability of Ti_3SiC_2 Thin Films," *Acta Mater.*, **55** [4] 1479–88 (2007).

[47]L. Farber and M. W. Barsoum, "Isothermal Sections in the Cr-Ga-N System in the 650-1000 °C Temperature Range," *J. Mater. Res.*, **14** [6] 2560–6 (1999).

[48]Y. Du, J. Schuster, H. Seifert, and F. Aldinger, "Experimental Investigation and Thermodynamic Calculation of the Titanium-Silicon-Carbon System," *J. Am. Ceram. Soc.*, **83** [1] 197–203 (2000).

[49]T. El-Raghy, S. Chakraborty, and M. W. Barsoum, "Synthesis and Characterization of Hf_2PbC, Zr_2PbC and M_2SnC (M=Ti, Hf, Nb and Zr)," *J. Eur. Ceram. Soc.*, **20** [14–15] 2619–5 (2000).

[50]T. El-Raghy and M. W. Barsoum, "Diffusion Kinetics of the Carburization and Silicidation of Ti_3SiC_2," *J. Appl. Phys.*, **83** [1] 112–9 (1998).

[51]T. El-Raghy, M. W. Barsoum, and M. Sika, "Reaction of Al With Ti3SiC2 in the 800–1000°C Temperature Range," *Mater. Sci. Eng. A*, **298** [1–2] 174–8 (2001). □